

Mimicking the large-scale structure of the Local Universe

Synthetic pre-labelled galaxies in large-scale structures

M. Alcázar-Layne¹, S. Duarte Puertas^{1,2}, S. Verley^{1,2}, G. Blázquez-Calero³, A. Jiménez¹, A. Lorenzo-Gutiérrez⁴, D. Espada^{1,2}, M. Argudo-Fernández^{1,2}, and I. Pérez^{1,2}

¹ Departamento de Física Teórica y del Cosmos, Facultad de Ciencias (Edificio Mecenas), Universidad de Granada, E-18071 Granada, Spain

² Instituto Carlos I de Física Teórica y Computacional, Spain

³ Instituto de Astrofísica de Andalucía, CSIC, Glorieta de la Astronomía s/n, E-18008 Granada, Spain.

⁴ ATG Analytical, Avda de Andalucía 5, Granada, Spain

Received June 26, 2025; accepted January 22, 2026

ABSTRACT

Context. Current observational and simulated large-scale structure (LSS) catalogues often lack consistency in assigning galaxies to specific structures, due to the absence of a universally accepted classification criterion.

Aims. With the aim to generate synthetic empirical data for fine-tuning LSS classification algorithms, as well as to train machine learning (ML) and deep learning (DL) models for the same purpose, this work presents a purely geometrical simulation based on the statistical spatial properties found in LSS surveys, using the spectroscopic main galaxy sample of the Sloan Digital Sky Survey (SDSS) catalogue up to a redshift of $z \simeq 0.1$ as a specific use case.

Methods. A parallelism between the LSS and the 3D Voronoi tessellation was utilised, in which the nodes, links, surfaces, and cells of the diagram correspond to clusters, filaments, walls, and voids, respectively. The simulation used random positions within voids as seeds for tessellating the 3D space. The resulting tessellation structures were then randomly populated with galaxies that adhere to the statistical properties of their observational respective structures. As the galaxies were generated, they were tagged with their corresponding structure.

Results. In each simulation, six LSS mock catalogues were generated, following the statistical behaviour observed in the SDSS catalogue, depending on the structure they belong to. In addition, the Malmquist bias and the redshift-space distortion, known as the Fingers of God (FoG) effect, were simulated as well.

Conclusions. We present a novel geometrical LSS simulator, where generated galaxies mimic the statistical properties of their observational belonging structure. As an example, the simulator was tuned to mimic the SDSS catalogue, although any other catalogue can be considered in similar studies. With the generated catalogue, it is possible to adjust the LSS classification algorithms, train and test ML and DL models, and benchmark several LSS classification methods using this pre-labelled data to compare and contrast their results and performance.

Key words. Methods: numerical – Surveys – Galaxies: clusters: general – Galaxies: distances and redshifts – large-scale structure of Universe –

1. Introduction

It is generally known that the environment of each galaxy affects its evolution. In recent decades, studies have revealed the extensive arrangement of galaxies, consisting of clusters, filaments, and walls, where galaxies are primarily grouped together as a result of gravitational attraction (Seth & Raychaudhury 2020; O’Kane et al. 2024; Van Kempen et al. 2024). In contrast, underdense, sparsely populated areas known as voids exist as well. There have been limited opportunities to study these structures until large galaxy surveys started mapping the Universe at large scales. The first attempt was the CfA Redshift Survey (Geller & Huchra 1989), which measured the radial velocities of galaxies brighter than 14.5 magnitudes and using the Hubble-Lemaître law to obtain the first 3D reconstruction of part of the Local Universe. Since then, numerous large-area surveys have been performed, based on huge samples of galaxies (e.g. Sloan Digital Sky Survey -SDSS-, York et al. 2000; 2dFGRS, Colless et al.

2001; VVDS, Le Fèvre et al. 2005; GAMA, Driver et al. 2011) and used to study these large-scale structures (LSSs; Gott et al. 2005; Pimbblet et al. 2004; Guzzo et al. 2014; Alpaslan et al. 2014, for SDSS, 2dFGRS, VIPERS, and GAMA, respectively) and the characteristics of galaxies within them. These studies have confirmed that such structures appear both in the Local Universe and at greater distances, noting that the structures resemble soap bubbles or spider webs. However, the Universe is more complex than this basic description and it might even present a hierarchical structure (Jaber et al. 2024).

Galaxies located in different structures present a wide range of characteristics. In an environment with nearby galaxies, which is common for clusters and filaments, gravitational forces work alongside other processes (e.g. ram pressure stripping and strangulation) to act as catalyst for star formation (e.g. Balogh et al. 1998, 2004; Lewis et al. 2002; Rines et al. 2005). Also, denser zones offer a hot intergalactic medium that also affects the evo-

lution and properties of galaxies. Due to these interactions, their gas is forced to collapse and form stars earlier than in galaxies located in voids or sparsely populated walls. [Dressler \(1980\)](#) studied this gravitational effect in galaxies in rich clusters, finding that the outer parts of the clusters are mostly composed of spiral galaxies with younger stellar populations than the elliptical and lenticular galaxies that tend to dominate in the inner parts of clusters. To study the influence of the LSSs over their galactic population, it is necessary to know the structure which these galaxies belong and their typical characteristics: morphology, colour, stellar mass, size, amongst others. To date, several catalogues of galaxy clusters have been compiled (e.g. [Abell et al. 1989](#); [Tempel et al. 2012, 2014b, 2017](#)), with a number of them based on SDSS data. For voids, we can refer to [Kreckel et al. \(2011\)](#) or [Pan et al. \(2012\)](#), and then to [Tempel et al. \(2014a\)](#) for background on filaments. Currently, there are no observational catalogues of walls available.

In general, cluster galaxies and inner void galaxies can be relatively easy to identify, however, in some cases, there are discrepancies between the classifications determined by different authors. For instance, due to the lack of a commonly accepted definition of the LSS, some authors might classify a galaxy in the frontier of a void as a void galaxy, while others might classify it as a wall or filament galaxy. There is no widely accepted and adopted criterion in the literature, which means that several existing structure-specific algorithms end up in contradiction with one another in a way that makes impossible to evaluate their consistency, when taken together or individually. For example, in [Neyrinck \(2008\)](#), a parameter-free void-finding method was developed to find a differential property that would allow for a cosmological standard definition of voids to be established. However, if the method is only focussed on a specific structure, we would have to use a range of different methods for all the others, presenting a potential discrepancy between these methods. In [Libeskind et al. \(2018\)](#), 12 cosmic web structure classification methods are visually and quantitatively compared to define an objective standard rule. As a result, they found that each algorithm captures different properties of the cosmic web, proving valuable in establishing the relationship between their results and the effect on galaxies. Although some authors have used N-body simulators to mimic the cosmic web and tune their algorithms, these simulations make no explicit reference to the structure to which each galaxy belongs, making it impossible to know exactly how reliable each method is. As explained in [Aragon-Calvo \(2019\)](#), training data for semantic segmentation must satisfy characteristics, such as establishing unique labelling systems that are consistent (i.e. the definitions of structures must be immutable across all data) and diverse (i.e. sufficiently representative to capture the full spectrum of the problem). This also applies to other ML-based methods and to mock testing data.

Due to this discrepancy, in this work, we present a geometrical LSS simulator that is based on the spatial properties of the galaxies present in LSS catalogues, according to their belonging structure, with well-defined sub-samples of galaxies belonging to voids, walls and filaments, as well as clusters. Mock galaxies were labelled at the time of their generation inside their corresponding structure, which makes the catalogue an accurate reference for fine-tuning the LSS classification algorithms, comparing and benchmarking their results against the empirical mock catalogue, and training both machine learning (ML) and deep learning (DL) models to find the defining features that allow us to differentiate between the galaxies of different structures.

The structure of this article is organised as follows. Section 2 presents the applied data, consisting of the catalogues we used

as a reference to extract the characteristics of each cosmic structure. In Section 3, we describe the initial conditions and methodology of the simulation of LSS galaxies in the mock universe, while the characteristics of a generated mock universe using this method are presented in Section 4. Their quantitative and qualitative features are inspected and compared with the reference catalogues in Section 5, along with several proposals for future improvements. Finally, a summary of this work and the main conclusions of this study are given in Section 6. In this work, a lambda cold dark matter (Λ CDM) cosmology is assumed, with $H_0 = 69.32 \text{ [km s}^{-1} \text{ Mpc}^{-1}\text{]}$, $\Omega_M = 0.287$, and $\Omega_\Lambda = 0.713$.

2. Data: Observational catalogues

As a practical application, in this work, the SDSS ([Alam et al. 2015](#)) data were considered as a general LSS catalogue which shape, biases and geometrical limits can be used as parameters to reproduce a synthetic observed universe in the simulator. In the present work, an indicator of the population and distribution of galaxies within each structure is required. To that aim, two different observational catalogues were used, namely, [Pan et al. \(2012\)](#) and [Tempel et al. \(2017\)](#), as described in brief below:

- [Pan et al. \(2012\)](#): a public catalogue of cosmic voids based on SDSS Data Release 7 (SDSS-DR7, [Abazajian et al. 2009](#)). The voids were extracted using the Void Finder method developed by [El-Ad et al. \(1996\)](#). This catalogue contains 79,947 galaxies distributed across 1055 voids.
- [Tempel et al. \(2017\)](#): to characterise clusters, the present work makes use of this galaxy groups catalogue, which contains 584,449 galaxies belonging to 88,662 groups.

There are several studies in the literature that investigate the distribution of galaxies in SDSS according to their structure, which can be used as a reference to set different values in the simulation configuration. For example, Fig. 8 of [Cautun et al. \(2014\)](#) presents a theoretical model estimating the volume and mass distribution of galaxies in the SDSS catalogue as a function of the structure in which they reside, according to the method applied by the authors. [Libeskind et al. \(2018\)](#) presented a comparison between twelve different methods to determine the volume and mass distribution in LSS, which will be contrasted and compared against the resulting mock universes to determine the goodness of the presented simulator in these values. Additionally, the application LSSGalPy developed by [Argudo-Fernández et al. \(2017\)](#) was used to visualise the LSS of the simulated mock catalogues in multiple space projections.

3. Methodology

Observational LSS catalogues show the spiderweb morphology that the Universe presents at large scales. There is a large number of geometric parameters that can be extracted from these structures: length of filaments, area of the walls, volume of voids, number of filaments intersecting in clusters, and others. In the same way, it is possible to obtain certain properties: number of galaxies per length, as well as the surface and volume units in filaments, walls, clusters and voids, respectively. Although there is no fixed number for these parameters, ideally, to create a mock universe only one single parameter is necessary: the volume of the Universe to be generated. Any other parameter (e.g. the number of galaxies) must be constant or only depend on this single parameter, presenting a statistical behaviour that every mock universe must fit and reproduce to generate the most

realistic data. All the parameters of the presented simulator only depends of the desired simulation size and are estimated following stochastic models described below.

3.1. 3D mock universe parameters

In the early Universe, mechanisms such as cosmic inflation established the initial conditions of the universe, such as homogeneity and isotropy. The existing irregularities in the early Universe resulted in a non-uniform mass distribution that established the footprint of the current galaxy distribution within it while it expanded (Sparke & Gallagher 2007). To generate mock universes similar to the observed one, we can make use of Voronoi tessellations. The Voronoi tessellation can be calculated by growing (or expanding) spheres radially from the positions of the generator points. The intersection of two or more spheres establishes the edges, surfaces, and vertices of the Voronoi tessellation for those generator points. With the Voronoi tessellation, it is possible to recreate the shape of the LSS, considering edges as filaments, surfaces as walls, vertices as galaxy clusters, and empty zones as voids. Using this interpretation, it is possible to generate random points representing galaxies along these structures, while controlling their density and location. In the literature, the Voronoi tessellation is widely used by some authors to study the LSS. For example, it was used by El-Ad & Piran (1997) to test void-finding algorithms populating a simulated universe with void and wall galaxies. Icke & van de Weygaert (1987); van de Weygaert & Icke (1989); Aragón Calvo (2007); Aragón-Calvo et al. (2010) used it to interpret the LSS, obtaining a consistent correlation with the observations. Furthermore, the Voronoi tessellation not only serves as a simulator back end, but also as a parameter estimation method. For instance, the Voronoi Tessellation was used in Neyrinck (2008) to estimate the local densities of galaxies and find void frontiers.

In the present simulator, filaments and walls are treated as the same structure because: i) there are no filament catalogues complete enough to extract scaling relationships or intrinsic properties characterising these structures to implement them in the present simulator; and ii) at the time of writing, edges in the Voronoi tessellation (scipy.spatial.Voronoi) from SciPy (Virtanen et al. 2020) are not well indexed for iterative processing. Specifically, For a given Voronoi cell, the edge was occasionally listed twice (populated with galaxies twice, doubling the filament density), while other times, an edge was never listed at all; as a result, no galaxies were generated for those unlisted filaments. Additionally, since this simulator produces a geometrical representation of the LSS without specifying the intrinsic properties of each galaxy, all simulated galaxies are generated with an unitary stellar mass. Despite these considerations, to build the main blocks of the simulator, it is necessary to characterise the following parameters:

- volume and shape of the generated mock universes;
- total count of structures: voids, clusters, walls and filaments;
- galaxy spatial distribution and density in each structure;
- know maximum and minimum sizes, areas, and volumes for each structure in the observed Universe.

As mentioned previously, in this work, the SDSS catalogue is used as the reference to extract these parameters as a case study. We note that the SDSS occupies $\sim 1/6$ of the complete sky. The simulator generates a whole-sky simulation and then it is cut into six slices with the shape of the SDSS, generating six mock universes at once. Thus, some parameters (such as the number of voids) will be scaled up according to this difference.

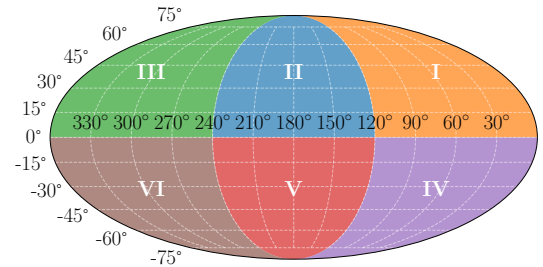


Fig. 1. Spatial limits of each generated mock catalogue. Each slice, represented with different colours, ranges 120° in R.A. and 90° in Dec., and expanding radially from 0 to 500 [h^{-1} Mpc].

All adjusted parameters and their values utilised for the SDSS use case are summarised in Table A.1.

The first parameter needed by the simulator is the size of the simulated universe. To generate the mock universes with a shape resembling the what is indicated by the SDSS 3D spatial data, sphere-shaped universes with a radius of 500 [h^{-1} Mpc] can be generated, corresponding approximately to a redshift of $z \simeq 0.1$. The majority of the SDSS catalogue data occupy from 120° to 240° in right ascension (R.A.) coordinates and from 0° to 90° in Declination (Dec.) coordinates. Taking into account this fact, this spherical whole-sky simulation is then sliced into six portions, giving six simulated mock catalogues with the same shape and volume as the reference one. In Fig. 1, we show the spatial extent of each slice.

The next parameter to determine is the number of voids to be generated, which is done at random within the volume of the simulation. Pan et al. (2012) found approximately 1000 voids in the SDSS catalogue. Scaling this parameter to the whole sky, in the present simulation, a number of $6 \times 1000 = 6000$ voids were set by default. However, other authors such as Mao et al. (2017) estimates the number of voids in catalogue around 1200. This discrepancy can be explained because of the differences defining void limits, as well as the irregular shape of cosmic voids, where (depending on the method used) the same void can be defined in sub-parts, increasing their total number. For example, in Douglass et al. (2023), the number of detected voids goes from 518 to 1184 depending on the method and cosmology used. Thus, in the present simulator, this parameter will vary between $6 \times [500, 2000] = [3000, 12,000]$.

3.1.1. Cluster galaxies density and distribution

The parameters needed to generate the cluster galaxies are the statistical distribution of the number of galaxies in a cluster, their spatial distribution, and the distortion in redshift space caused by the dispersion in their radial velocities due to the random peculiar velocities of galaxies within them, known as the Fingers of God (FoG) effect. In the case of clusters, it is difficult to determine the cluster galaxy density for several reasons. For instance, there are faint galaxies that cannot be resolved optically or distinguished from other kinds of object, leading to uncertainty when trying to define physical boundaries of clusters and their shapes (let alone the spatial redshift distortion). Nevertheless, for the purposes of this work, this parameter was estimated to obtain an initial value, which could then be modified in case the differences between the cluster simulation and the reference catalogues were, in fact, clearly seen.

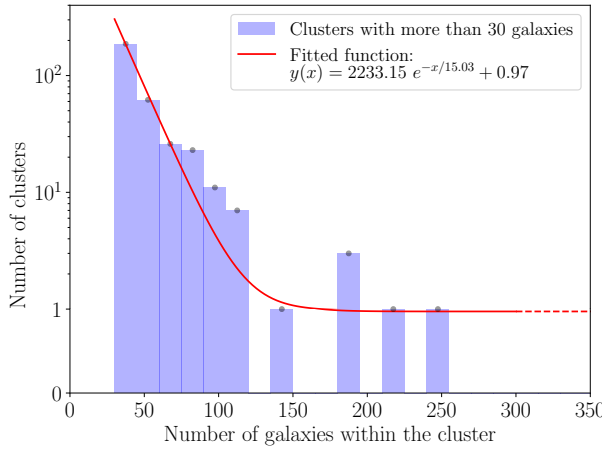


Fig. 2. Count of clusters as a function of their number of galaxies in the reference catalogue of Tempel et al. (2017). Blue bars indicate the count of clusters. Red line indicates the fitted function over the data from the reference catalogue (used in the default configuration).

The typical stellar masses of clusters of galaxies are $\sim 10^{13} - 10^{15} M_{\odot}$ and their radii are of the order of 1-4 Mpc.

Assuming that each galaxy has a mean stellar mass of $\bar{M}_{\star} \simeq 10^{11} M_{\odot}$ and considering a typical cluster stellar mass of $M_{\text{cluster}} \simeq 10^{14} M_{\odot}$, the expected number of galaxies in a cluster is $n = 1000$ galaxies. Assuming a typical spherical cluster with radius 2 Mpc, the mean density, η , is expressed as

$$\eta = \frac{n}{4/3 \times \pi \times 2^3 [(\text{h}^{-1}\text{Mpc})^3]} = 29.8 \approx 30 \text{ [galaxies/}(\text{h}^{-1}\text{Mpc)}^3\text{].}$$

Although this number can be used, it might be meaningless, as due to gravitational attraction, there are more galaxies in the inner radius than in the outer ones. Additionally, considering spherical shapes for clusters, at a given radial range, the volume is smaller in the inner zones than the outer ones. These two effects make the spatial distribution highly inhomogeneous, as discussed in Appendix C. In the present simulator, instead of just assuming a uniformly distributed random galaxies within a simulated cluster given a density, the number of galaxies for each cluster is chosen with a user-selectable probability distribution. Then, this number is used to give the synthetic cluster a maximum radius as a function of its number of galaxies, also chosen randomly with a distribution specified by the user. For these two parameters (number of galaxies and maximum radius), four kinds of distributions can be selected: a Gaussian one, such as the Navarro-Frenk-White (NFW; Navarro et al. 1996, 1997) and Einasto (Einasto 1965) profiles, or a SDSS-like distribution that follows the behaviour of the clusters found in the catalogue. By default, the SDSS-like distribution is used in all parameters, but this can be changed in the configuration file provided with the software.

As often found in the literature, a group of galaxies with 30 or more systems is considered a cluster (Abell et al. 1989). Also, in the SDSS catalogue, the most populated cluster contains ~ 300 galaxies. These two indicators can guide us when we are trying to limit the number of galaxies in the synthetic clusters. A prior study on the distribution of the number of cluster galaxies in SDSS was carried out using data from Tempel et al. (2017), resulting in the distribution shown in Fig. 2. Considering the minimum and maximum number of galaxies found in SDSS clusters, we can fit an exponential function to build up a probability

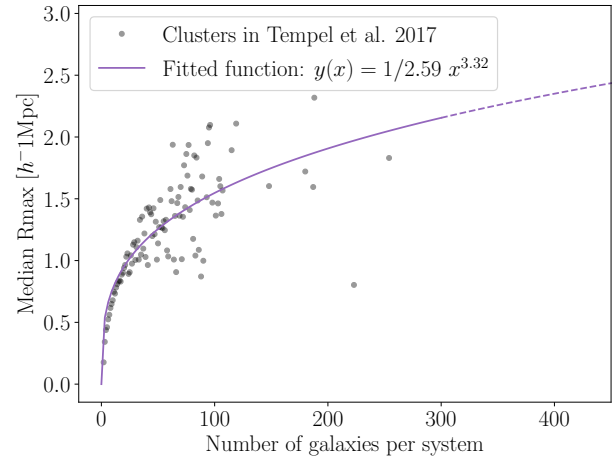


Fig. 3. Maximum radius of clusters as a function of their number of galaxies in the reference catalogue. Black dots indicate the clusters from Tempel et al. (2017). Purple line indicates the fitted function over the reference catalogue data.

density function $P_{n_i, C_i}(x)$ to feed the synthetic cluster generation code,

$$P_{n_i, C_i}(x) = \frac{1}{4822.50} (2233.15 \times e^{\frac{-x}{15.03}} + 0.97), \quad x \in [30, 300],$$

where C_i is the cluster number i and n_i is the number of galaxies in that cluster. In addition to the number of galaxies, the radius of clusters (i.e. the dispersion of the distance between a cluster galaxy and its cluster geometric centre) can also follow either a Gaussian distribution or a SDSS-like one. As shown in Fig. 3, for the SDSS-like distribution, a study of the distribution of the radius of clusters as a function of their number of galaxies in SDSS was carried out using data from Tempel et al. (2017), following

$$R_{\text{max}, C_i}(n_i) = \frac{1}{2.59} n_i^{1/3.32} [\text{h}^{-1}\text{Mpc}].$$

Here, C_i is the cluster number i and n_i is the number of galaxies in that cluster. Values below 0 or above 4 [h^{-1}Mpc] are discarded and another random number is injected until the value reached between [0, 4]. The next parameter aims to recreate the radial velocity dispersion bias (also known as the FoG effect) when observing physically bound dense areas. This effect solely depends on the local density. A limited study on the velocity dispersion in clusters as a function of their number of galaxies (i.e. the local density) in SDSS was made using data from Tempel et al. (2017) by fitting the median of the velocity dispersion for each specific number of galaxies in groups. The results, plotted in Fig. 4, were obtained via

$$\sigma_{v, C_i}(n_i) = -585.40 \times e^{-n_i/59.49} + 804.71 [\text{km/s}],$$

where C_i is the cluster number i and n_i is the number of galaxies in that cluster. Once $\sigma_{v, C_i}(n_i)$ is computed, a random radial displacement is applied to each galaxy of cluster C_i using a normal distribution with $\mu = 0$ and $\sigma = \sigma_{v, C_i}(n_i)$.

3.1.2. Wall and filament galaxies configuration

These two structures need to be treated together: when two walls intersect, the region where these structures cross is approximately equal to the sum of the densities of each intersecting wall. This is why – despite the fact that it is not possible

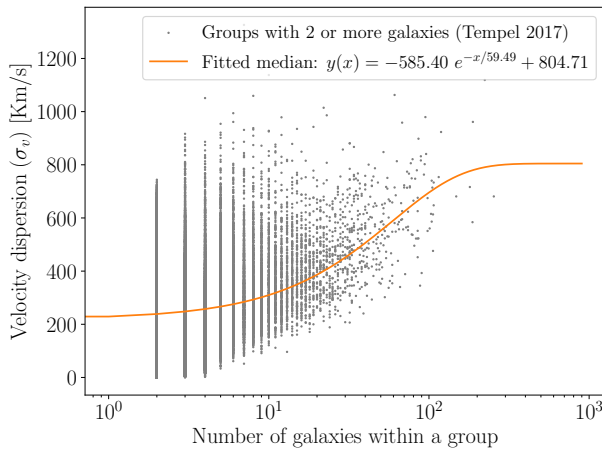


Fig. 4. Fitted function for the FoG effect using Tempel et al. (2017) data. Black dots indicate groups in the reference catalogue. Orange line indicates the fitted function over the reference data.

to control the density of filaments and walls separately – it is possible to adjust the densities of these structures based on our knowledge of this effect and reach the densities of the filaments and walls from the observed Universe. Despite the controversy around defining filaments and walls, due to the fact that the number of galaxies in these two regions represents approximately 80% of the entire Universe, it is assumed that the wall and filament structures are characterised by the same mean galaxy density than the Universe, which correspond to approximately $0.1 [\text{galaxies} \times (\text{h}^{-1}\text{Mpc})^{-3}]$. In the outer parts of the Voronoi tessellation, larger cells are generated due to the lack of boundary generator points and, thus, immense computer-intensive walls and filaments will be populated. To dispose of them, a wall area limit can be programmed to avoid having to populate walls and filaments above this limit. Taking all this into account, the parameters needed to configure the wall and filament galaxy generation procedure are as follows:

- surface density of galaxies in walls per $[\text{h}^{-1}\text{Mpc}]^2$;
- maximum area of walls in $[\text{h}^{-1}\text{Mpc}]^2$;
- distribution in the spatial separation of galaxies from the plane of their assigned wall;
- parameters of the chosen distribution (mean, dispersion, ...).

The spatial separation parameter can be configured to follow a Gaussian or a uniform distribution. The Gaussian distribution can be configured in mean and dispersion, set with $\mu = 0 [\text{h}^{-1}\text{Mpc}]$ and $\sigma = 0.5 [\text{h}^{-1}\text{Mpc}]$ as the default. For the uniform distribution, low and high values of $-0.5 [\text{h}^{-1}\text{Mpc}]$ and $0.5 [\text{h}^{-1}\text{Mpc}]$, respectively, were set. By default, it is assumed that the spatial separation of galaxies from their wall plane follows a normal (Gaussian) distribution.

3.1.3. Void galaxies density and distribution

In the present simulator, the user can select how to determine the number of void galaxies for each simulation among these three options:

- by density: generate a specified number of void galaxies per volume;
- by ratio: generate a specified number of void galaxies following the proportion with the number of galaxies from the other structures;

- fixed: specified number of void galaxies in the whole simulation, regardless of any other parameter.

To establish a number of void galaxies using the density method in each simulation, Pan et al. (2012) estimates a density of $0.01 [\text{galaxies} \times (\text{h}^{-1}\text{Mpc})^{-3}]$. This number matches the Calar Alto Void Integral-field Treasury survey (CAVITY, Pérez et al. 2024) project results, obtaining approximately the same density value for almost every studied void in its first public data release (García-Benito et al. 2024).

Moreover, instead of using the density of voids, once galaxies in other structures have been generated, we can estimate the number of void galaxies needed to follow the mass proportions by structure. According to Pan et al. (2012), it is known that void galaxies represent about the 10% of the total of galaxies in the Universe. However, other works have reported different percentages. For example, following the theoretical models of Aragón Calvo (2007) and Cautun et al. (2014), this number can vary from 15% to 26%. According to other theoretical results, such as those from the studies compared in Libeskind et al. (2018), the portion of void galaxies in the LSS can vary from 10-15% to $>50\%$ depending on the method, according to their simulations. By default, the simulator computes the number of void galaxies using this last method (by ratio) with a default value of 15% of void galaxies. The final configurable parameter in void galaxies generation is the method used to populate the space: i) populating the entire volume with void galaxies (regardless if they are generated inside other structures, thereby polluting them and inducing positional noise in the generated dataset); and ii) populating only under-dense areas given a configurable threshold.

3.2. 3D mock universe generation

We performed a 3D Voronoi tessellation procedure, where a specified number of random points were spread between the given simulation spatial limits using a uniform distribution. Once the tessellation was done, the different structures were split and populated with galaxies independently.

The next step was to populate the generated regions with mock galaxies. Following the Voronoi tessellation, in the mock model clusters can appear where two or more filaments intersect (see Fig. D.1), namely, in tessellation nodes. Hence, for some nodes, random points (galaxies) are generated and randomly distributed around them. The number of points follows the distribution set in the configuration. The next algorithm shows how each cluster is populated with galaxies:

Algorithm 1 Cluster galaxy generation algorithm

```

for each cluster  $C_i$  do
  Determine random number of galaxies  $nOfGal$ 
  Determine maximum radius  $rmax$  as a function of  $nOfGal$ 
  Generate  $nOfGal$  random points in a spherical distribution of radius  $rmax$ 
  Translate the random points sphere to  $C_i$  cluster centre
  If selected, apply FoG effect by distorting the redshift of the galaxies
end for

```

Galaxies in walls and filaments have to be synthesised in four steps. The steps needed to generate the wall and filament galaxies are as follows: i) obtain each cell in the tessellation; ii) extract each face of the cell and, via an affine transformation, reduce the dimension of the face to a 2D face; iii) add uniformly randomly

disposed points in this 2D face along its x and y coordinates, ensuring the points are inside the face, then apply a random z coordinate with a Gaussian distribution to each one; and iv) reverse the affine transformation made previously both for the face and for every generated point, then update the mock dataset with this new set of generated mock galaxies. This steps are schematised in the following algorithm:

Algorithm 2 Wall and filament galaxies generation algorithm

```

for each wall  $W_i$  do;
    Reduce the dimension of  $W_i$  to XY plane to get a flat 2D
    polygon.
    Compute area of wall  $areaW_i$ .
    Compute number of galaxies  $nOfGal$  as a function of the
    configured density and  $areaW_i$ .
    Generate  $nOfGal$  random points distributed in the flat 2D
    polygon.
    Give each point a random Z coordinate.
    Restore the 3D dimension of  $W_i$  containing the random
    points.
end for

```

By repeating this algorithm for each face of a region, it is possible to obtain the mock void with its enclosing walls and filaments galaxies, as shown in Fig. D.2. The generation of void galaxies presents several challenges for which design decisions have had to be made. It is possible to just generate random points as mock void galaxies along the mock universe, no matter which specific void each galaxy belongs to. However, if there is no control over the coordinates where void galaxies are generated, they could grow inside another region, thereby injecting categorisation errors into the mock universe and into the processes that could be fed with it. Thus, a density-driven method was developed to generate void galaxies in under-dense areas exclusively, which is determined by a given threshold in the configuration file. Once all the galaxies of the others structures have been generated, a 3D histogram is performed, resulting in the count of galaxies per voxel. Then, the histogram is inverted, where the voxels with the maximum count of galaxies will contain the value of '0' and the voxels that previously had zero galaxies will now contain the maximum value of the previous histogram. This inversion offers a direct density map of the positions to generate the void galaxies. A graphical example is shown in Fig D.3 representing the inverted histogram extracted during the generation of a random mock universe. If the user opts to populate the entire space with void galaxies (regardless of whether it pollutes other structures), random points are created within the mock universe using a uniform distribution. In the opposite case, the user can select to populate only the under-dense areas, for which the following method is applied:

Algorithm 3 Void galaxies generation algorithm

```

Generate a voxelised probability histogram of the current
mock universe, with clusters and walls already populated.
Invert the probability of each voxel by doing
 $P_{Void} = 1 - P_{Cluster,Wall}$ .
Generate  $nOfGal$  random points.
Distribute the random points using the inverted probability
histogram as a density map.

```

In any case, the generation of void galaxies is uniformly distributed. Thus, a constant density of void galaxies is expected, which does not depend on the distance to the centre of voids

(in line with Pan et al. 2012). The use of this method results in the galaxy spatial distribution shown in Fig. D.4, which is being simplified to two dimensions for the sake of clarity. In the figure generated uniformly distributed void galaxies avoids to appear in dense areas. We can also clearly see how computing the void zones using voxels results in irregular wall fitting, presenting that distinctive triangular frontier near walls, which illustrates an extreme staircase effect: voxelisation artifacts in computational geometry and 3D modeling when a continuous shape, such as a sphere, is represented using discrete elements such as voxels. Because voxels have a cubic shape and cannot provide a perfect fit to curved surfaces, the process introduces volume errors and surface irregularities. As illustrated in Fig. D.5, the induced error decreases proportionally with smaller voxel sizes.

3.3. Mass and volume distribution of structures

There are several characteristics that need to be measured in the mock catalogues once all galaxies have been generated. These are used to analyse, compare, and ensure agreement between these catalogues with the observational ones. According to the stellar mass distribution, we assumed that galaxies have a unitary mass. Thus, the total stellar mass of the mock universe is computed as the sum of all the generated galaxies. The distribution of stellar mass is calculated as the total stellar mass of the galaxies of a particular structure divided by the total stellar mass of the mock universe, expressed as

$$M_{Total} = M_{Cluster} + M_{Wall,Filament} + M_{Void}; \quad (1)$$

$$P_{Cluster} = \frac{M_{Cluster}}{M_{Total}} [\%]; \quad (2)$$

$$P_{Wall,Filament} = \frac{M_{Wall,Filament}}{M_{Total}} [\%]; \quad (3)$$

$$P_{Void} = \frac{M_{Void}}{M_{Total}} [\%]; \quad (4)$$

where M_{Total} , $M_{Cluster}$, $M_{Wall,Filament}$, and M_{Void} correspond to the total stellar mass of the simulation and the cumulative sum of the clusters, the walls and filaments, and the voids stellar masses, respectively. Here, $P_{Cluster}$, $P_{Wall,Filament}$, and P_{Void} represent the portion of the total simulated stellar mass represented by clusters, walls and filaments, and voids, respectively.

Due to the difficulty in defining the LSS and their limits, the volume estimation of the structures is not trivial. There exists several methods that can be applied to a specific structure and then these results can be compared and added to estimate the total volume. In the present simulator, the following methods are implemented:

For clusters:

- Sigma methods: each cluster is assumed to occupy the volume of a sphere that contains 95.45%, 98.76% and 99.73% (2σ , 2.5σ , and 3σ , respectively) of its galaxies.
- Convex hull method: the volume of each cluster is the same of a polyhedron envelope tangential to the most external galaxies, enclosing them all.

For walls and filaments:

- Sigma methods: each wall is assumed to occupy the volume of a polyhedron with the wall as its base and roof, parallel

between them, and a given height that makes the polyhedron enclose the 95.45%, 98.76%, and 99.73% (2σ , 2.5σ and 3σ , respectively) of its galaxies.

- Convex hull method: the volume of each wall is the same of a polyhedron envelope tangential to the most external galaxies, enclosing them all.

For voids:

- Voxel method: the simulation volume is divided in voxels. For each voxel, if the count of galaxies of other structures is less than the mean density, the voxel is assumed to be a void one. The total void volume is the sum of all void voxels volume. This method is highly dependent on the voxel size due to the staircase effect.
- Indirect method: Knowing the total cumulative volume of clusters, and walls and filaments, the total void volume can be calculated by subtracting them from the total simulation volume as $V_{Void} = V_{Total} - V_{Wall,Filament} + V_{Cluster}$.

Sigma estimation methods are common in the literature (see [Libeskind et al. 2018](#)). These operations present some caveats: different methods could show disagreement in their results; for example, by interpreting a spatial region as belonging to two structures, counting this space twice and therefore overestimating the total volume. In the same way that this work aims to establish a single method to classify all structures, the volume estimation should also be computed using a structure-independent single method. In the present work, the voxel method is expanded to cover all structures: the simulated volume is divided into voxels. For each voxel, if the count of galaxies of a specific structure is greater than the count of the others, the voxel is assumed to belong to this structure. If there are no galaxies within the voxel, it is added to the void structure. The total volume of each structure is the sum of all voxels volume of a given class. In case of a tie, the space of the voxel is divided by the number of tied classes. As noted before, this method is highly dependent on the voxel size due to the fact that (using the default configuration) the shape of the simulated universe is spherical. When voxels are used to divide the volume of a sphere, sampling errors that are inversely proportional to the voxel size are present: the smaller the voxel, the closer the sum of voxels volume is to the volume of the sphere. This staircase effect is illustrated in Fig. D.5 in the appendix.

3.4. Generating the output dataset

Before the spherical simulated catalogue was divided into six parts (as detailed before), the Malmquist bias was simulated and applied as well, where randomly selected galaxies were discarded from the simulation as a function of the distance. The aim here was to mimic the fact that there are faint galaxies difficult to detect optically. The more distant, the more undetectable galaxies, thus the number of detected galaxies decreases with the distance. This bias requires a reference, for which (in this use case) the SDSS catalogue was utilised to follow its distribution of galaxies along the distance to the observer, as represented in Fig. 8. This effect was implemented as follows. First, a histogram of the galaxy count per inverse- h megaparsec along the distance to the observer was created for both the reference and the mock catalogues. As the observational catalogue only occupies $\sim 1/6$ of the full sky, the observational count was multiplied by 6. Then, randomly chosen galaxies are discarded in mock universe for each $h^{-1} \text{Mpc}$ until both the observational and mock

galaxies counts at that distance were equal. Discarded galaxies are shown as the value ‘0’ in the ‘selected’ column, while the observable ones count with an ‘1’ in this column. As an exception, the parameters of cluster galaxies and their probability distributions were obtained from the observable Universe; therefore, these parameters were measured after they were affected by the Malmquist bias. Thus, cluster galaxies were excluded from the random selection of galaxies to be discarded. To mitigate this, the number of Voronoi nodes populated as clusters is decreased with the distance to the observer in the same proportion, as done in [Tempel et al. \(2017\)](#).

All the explained methods were implemented using [Python Core Team \(2019\)](#) v3.11 programming language for the program logic, [SciPy \(Virtanen et al. 2020\)](#) for generating the Voronoi tessellation of the simulated space (`scipy.spatial.Voronoi`), [Astropy \(Astropy Collaboration et al. 2013, 2018, 2022\)](#) for handling astronomical coordinates (`astropy.coordinates.SkyCoord`), and [NumPy \(Harris et al. 2020\)](#) and [Pandas \(pandas development team 2020; McKinney 2010\)](#) for structuring and handling the large amounts of generated data. The preliminary versions of the code before optimisations were tested using PROTEUS, the supercomputing centre of Institute Carlos I in Granada, Spain. After optimisations, the simulator can run on regular computers¹.

4. Results

We generated several random mock universes. Each one lasted about twenty minutes using a laptop with 64GB of RAM and a Intel i7 CPU with 16 logic cores. All realisations were produced using the same procedure to ensure they would be statistically consistent with one another. Thus, for the sake of clarity, the results of a single randomly chosen mock universe and its six slices (see Fig. 1) are featured. A representation of slice II is shown in Fig. 6. All results were measured after applying Malmquist bias. The symbol “ \pm ” represents the standard deviation of measured values (1σ).

The studied mock catalogue ranges from 0° to 120° , 120° to 240° , and 240° to 360° in R.A. and from -90° to 0° and 0° to 90° in Dec. The farthest galaxy is $\sim 500 [h^{-1} \text{Mpc}]$. The total volume of the mock universe is $523,598,776 [h^{-1} \text{Mpc}]^3$, where each slice occupies $87,266,463 [h^{-1} \text{Mpc}]^3$. The number of galaxies of each slice are $498,943 \pm 5142$. The mean density of galaxies in the studied mock is $\eta_{mock} = mass_{mock}/volume_{mock} = \sim 0.0057 [\text{galaxies} \times (h^{-1} \text{Mpc})^3]$. On average, the mass distribution of galaxies depending on their structure are organised as follows: 3.29% of galaxies belongs to clusters, 80.80% of galaxies belongs to walls and filaments, and the remaining 15.91% of galaxies belongs to voids, as illustrated in Fig. 7. The volume distribution result as follows: 0.07% of the volume of the mock universe belongs to clusters, 19.33% of the volume belongs to walls and filaments, and the remaining 80.60% of the volume belongs to voids. The Malmquist bias was simulated as well, with the result presented in Fig. 8, where galaxies follow the detection curve present in the reference catalogue.

4.1. Mock cluster properties

Each slice of the studied mock catalogue has $16,406 \pm 832$ cluster galaxies distributed in 333 ± 17 clusters, where each

¹ The code of the presented simulator is open source and publicly available at <https://gitlab.com/astrogal/mocklss>.

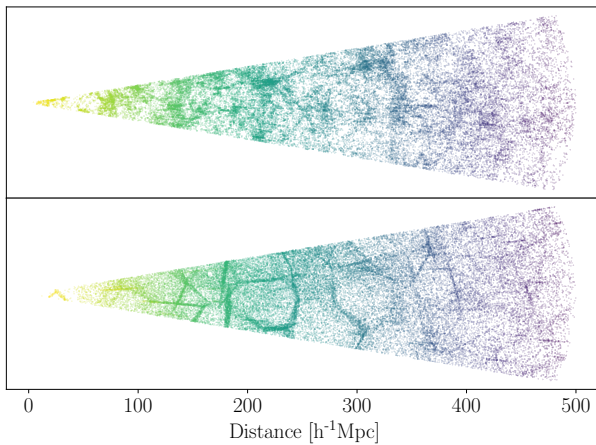


Fig. 5. Light cone comparison between a 15° sections of the reference SDSS catalogue (Alam et al. 2015) in the top panel and the analysed mock catalogue in the lower panel. Colour represents the distance to observer (the darker the purple shade, the farther the distance).

one of them contains 30 or more galaxies. The distribution in the number of galaxies within clusters is shown in Fig. 9. Depending on this number, each cluster presents differences in their radii (as seen in Fig. 10) and in their velocity dispersion (see Fig. 11). The mean density of galaxies is $\eta_c = 0.267 \pm 0.014$ [galaxies \times ($h^{-1}\text{Mpc}$) $^{-3}$]. The most populated cluster contains 291 galaxies. The number of connected filaments per cluster is four in all cases.

4.2. Mock wall and filament properties

The slices of the generated mock catalogue contains $403,150 \pm 7643$ wall and filament galaxies distributed in $15,022 \pm 569$ walls or filaments. As walls and filaments represents 19.33% of the total volume of the simulation, the total volume of wall and filaments in the studied mock universe is about $16,868,607$ [$h^{-1}\text{Mpc}$] 3 in each slice. The mean density of galaxies in walls and filaments has the value of $\eta_{w\&f} = 0.024 \pm 0.0001$ [galaxies \times ($h^{-1}\text{Mpc}$) $^{-3}$]. The most populated wall has 358 galaxies.

4.3. Mock void properties

Each slice of the generated mock catalogue has $79,386 \pm 3272$ void galaxies distributed in 1060 ± 37 cosmic voids. Voids represent the 80.60% of the total volume of the simulation, making a total volume of $70,336,769$ [$h^{-1}\text{Mpc}$] 3 in each mock universe slice. The mean density of galaxies within void has the value of $\eta_v = 0.001 \pm 0.00005$ [galaxies \times ($h^{-1}\text{Mpc}$) $^{-3}$]. This represents one-sixth of the mean density of galaxies in the mock universe.

5. Discussion

In this section, the characteristics of an arbitrary random mock universe are compared with reference catalogues. The results can vary for other simulated mock universes that use a different random seed, but their values are similar to those shown in this section. These studied features are summarised in Table B.1.

A visual inspection allows us to check that the simulated galaxies are labelled with their corresponding structure (as illustrated for slice II within $\text{R.A.} \in [120, 240]$, $\text{Dec.} \in [0, 90]$ in

Fig. 6). Also, Fig. 5 shows the filamentary structure of the simulation that is also given in the SDSS catalogue. Once inspected, the following statistical analyses are performed and contrasted with the reference catalogues. The total number of galaxies in the studied slices is $498,943 \pm 5142$. Within a footprint, common for both simulated and observational catalogues ($\text{RA} \in [140^{\circ}, 230^{\circ}]$, $\text{DEC} \in [0^{\circ}, 50^{\circ}]$ and $\text{Dist.} \in [100, 500]$ [$h^{-1}\text{Mpc}$]), the mock universe presents $275,487 \pm 6700$ galaxies, which is close to the reference SDSS catalogue, containing 274,975 galaxies.

The mass distribution of galaxies depending on their structure are organised as follows: 3.29% of galaxies belong to clusters, 80.80% of galaxies belong to walls and filaments, and the remaining 15.91% of galaxies belong to voids, as illustrated in Fig. 7. These mass and volume proportions are consistent with the results from other studies, such as Aragón Calvo (2007) and Cautun et al. (2014). In Libeskind et al. (2018), the algorithms of these and other authors are compared. Comparing the mock universe proportions with these studies, in general, this mock universe generator is able to keep these proportions when replicating the reference observational catalogue. However, the overall mass in clusters is lower than the estimations over the observational catalogue (discussion in Sect. 5.1). The Malmquist bias was also simulated, with the result presented in Fig. 8. When the number of galaxies in the mock universe is greater than in the reference catalogue for a given distance, randomly chosen ones gets discarded until the detection curve of both catalogues match. In this simulation, this occurs at ~ 150 [$h^{-1}\text{Mpc}$].

The features that we ought to measure next are specific to each structure. Due to the lack of wall and filament catalogues, it is not possible to contrast the characteristics in these two structures against observational data. In the following sub-sections, the properties of each specific mock structures are discussed.

5.1. Cluster properties

The studied mock catalogue has $16,406 \pm 832$ cluster galaxies per slice distributed throughout 333 ± 17 clusters, where each of them contains 30 or more galaxies. These values are close to those obtained in the catalogue of Tempel et al. (2017), which contains 16,419 cluster galaxies distributed throughout 322 clusters. The fraction of cluster galaxies in the mock catalogue is slightly lower than that obtained with the methods presented in Libeskind et al. (2018). This occurs for several reasons. First, the simulator produces galaxies with unitary mass, thus there are no galaxies within clusters with more mass than in other structures. Second, the number of clusters in the studied mock catalogue can deviate from the imposed distribution (see Fig. 9). This is a purely random effect: in other simulations, it can be greater than the fitted function. Third, this simulation is programmed to follow Tempel et al. (2017) catalogue, which essentially has a smaller number of cluster galaxies than that of Libeskind et al. (2018). Finally, the simulator generates clusters, namely, groups of galaxies with more than 30 galaxies. The methods presented in Libeskind et al. (2018) detect knots, which do not necessarily contain 30 or more galaxies. Because the simulation uses an isotropic Poisson-Voronoi 3D tessellation, the number of connected filaments per cluster is equal to the vertex degree of the tessellation (4), which matches the expected behaviour.

As seen in Fig. 9, the mock universe simulator is in line with the probability curve of the reference cluster catalogue when we are selecting a random number of galaxies for populating each one. In addition, depending on the selected number of galaxies, a maximum radius for each cluster is determined, which also follows the statistical behaviour found in the observational cat-

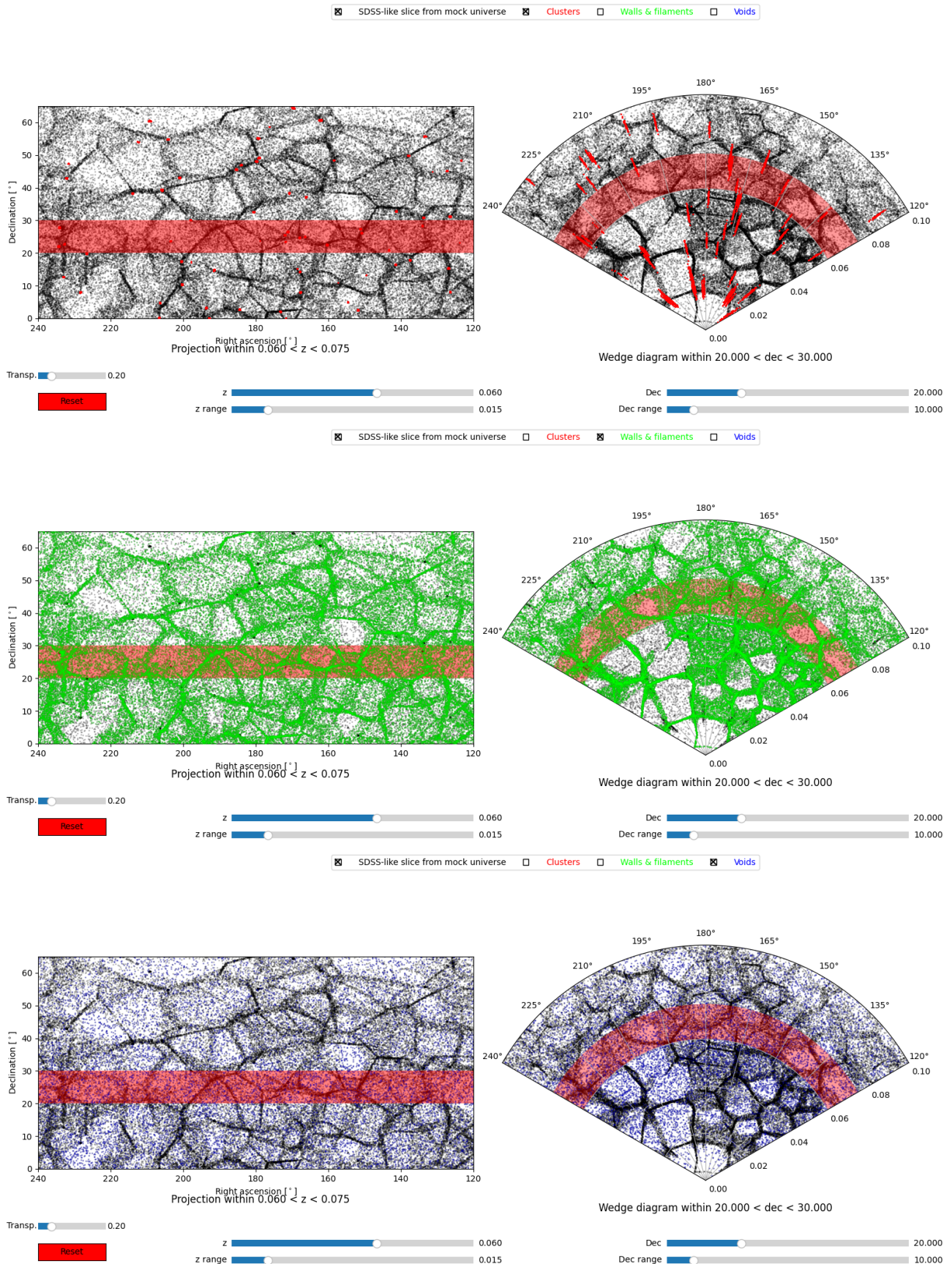


Fig. 6. SDSS-like slice II from a randomly generated mock universe. From top to bottom: Mock catalogue with cluster, wall and filament, and void galaxies coloured in red, green, and blue, respectively. In all panels, the red bands represent the range of redshift and declination shown. Upper panel: Mock catalogue with cluster galaxies coloured in red. Middle panel: Mock catalogue with wall and filament galaxies coloured in green. Lower panel: Mock catalogue with void galaxies coloured in blue.

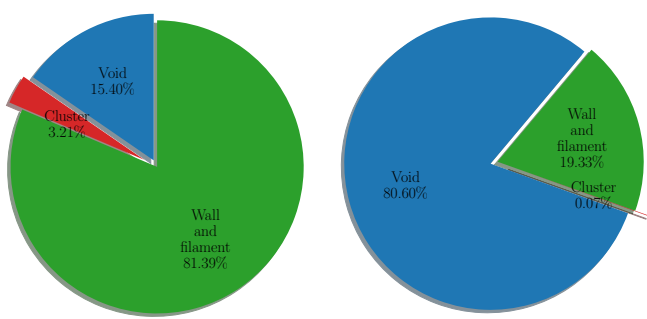


Fig. 7. Mass (left panel) and volume (right panel) distribution of galaxies per structure in the studied mock universe. The colour determines the structure as in Fig. 6.

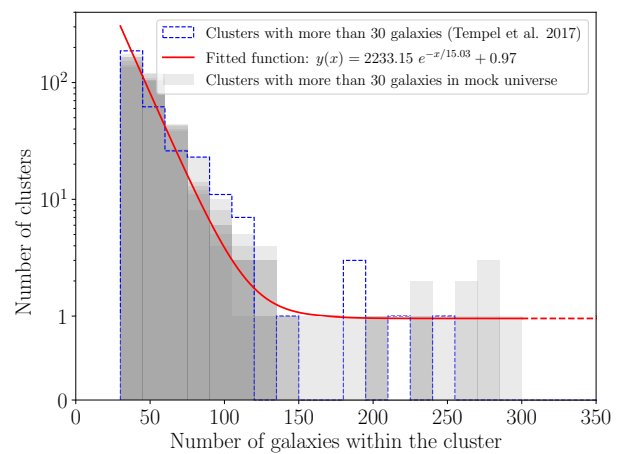


Fig. 9. Count of clusters as a function of their number of galaxies in Tempel et al. (2017) and in the simulated mock universe. Dashed blue line shows the number of clusters in Tempel et al. (2017). Red line shows the fitted function over the data from the reference catalogue. Grey bars show the number of clusters in each slice of the studied mock catalogue.

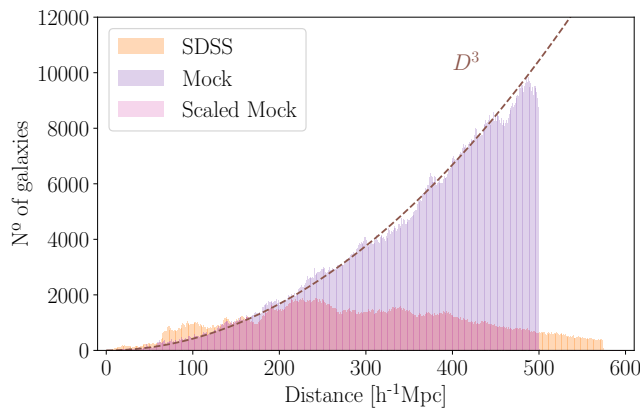


Fig. 8. Simulated Malmquist bias. Orange histogram shows the distribution of the number of sampled galaxies in the observational reference catalogue along the distance from origin. Purple histogram shows the distribution of the number of generated mock galaxies in the mock catalogue along the distance from origin. Pink histogram shows the distribution of the number of the selected mock galaxies in the mock catalogue along the distance from origin, after discarding some mock galaxies randomly to follow the behaviour of the observational catalogue. Brown dashed line gives the expected number of galaxies for a constant volume density of galaxies within the universe.

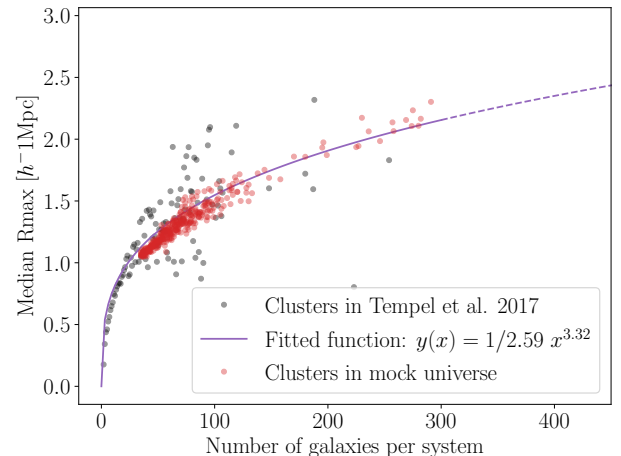


Fig. 10. Comparison between the maximum radius of clusters as a function of their number of galaxies in Tempel et al. (2017) (black dots) and in all slices of the generated mock universe (red dots).

atalogue, as shown in Fig. 10. The FoG effect was recreated successfully in the mock universe, where the cluster galaxies present a radial velocity dispersion that is dependent on the number of galaxies (a proxy of the total stellar mass) within their belonging cluster (as seen in Fig. 11), following the fitted curve shown in Fig. 4.

5.2. Void properties

The generated mock catalogue has $79,387 \pm 3272$ void galaxies distributed across 1060 ± 37 cosmic voids per each slice. These numbers are consistent with those presented in Pan et al. (2012), where 79,947 void galaxies distributed in 1054 voids were reported in the observational SDSS catalogue. In this reference void catalogue, the mean density of galaxies in voids represents the 10% of the mean density of the SDSS catalogue, rising from 20% to 100% near the borders of voids. In this simulation, the mean density of galaxies in voids is about 0.0010 ± 0.00001 [galaxies \times ($h^{-1}\text{Mpc}$) $^{-3}$], which represents the $\sim 18\%$ of the mean density of the studied mock universe and match the results of

the reference void catalogue. Moreover, the density of the mock void galaxies is uniform and not changing by the distance to the void centre, which replicates the observed behaviour of the void galaxies from the SDSS catalogue.

5.3. Wall and filament properties

The mean walls and filaments galaxy density is about four times the mean density of the whole mock catalogue, which is far from that of the clusters and voids (4700% and 18% of the mean density). This is expected when the distribution of mass per structure is taken into account because wall and filament galaxies represent approximately the 80% of the total mass of both mock and observational catalogues. Thus, it is expected that the mean density of the wall and filament would be about the same order of magnitude as the mean total density. Compared to Libeskind et al. (2018), the wall and filament mass fractions are expected

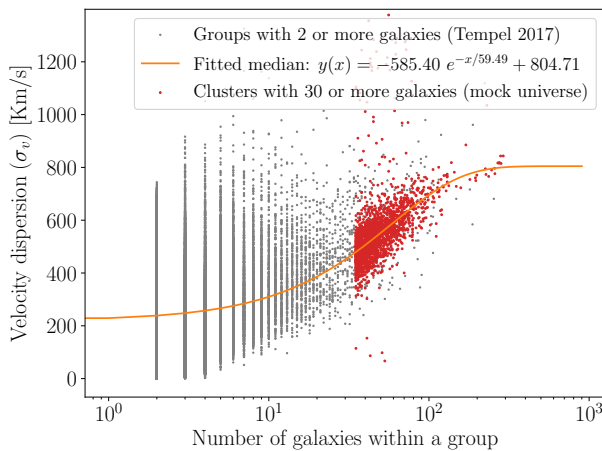


Fig. 11. Comparison between the radial velocity dispersion bias as a function of the number of galaxies in groups in Tempel et al. (2017) (black dots) and in all slices of the generated mock universe (red dots), which follows the fitted function over the reference catalogue data (orange line).

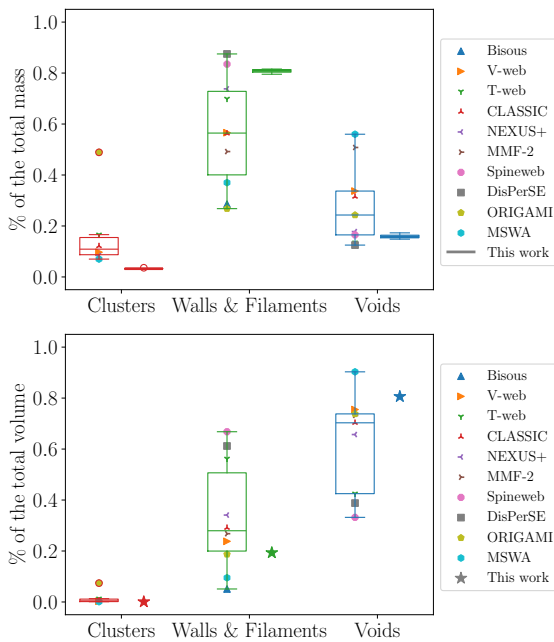


Fig. 12. Mass (upper panel) and volume (lower panel) distribution of galaxies depending on their belonging structure, comparing the data of the analysed mock universe against the results of the methods compared in Libeskind et al. (2018) over observational SDSS data.

to be above the mean, since galaxies in groups that are not classified as clusters fall into this category.

Observational catalogues of filaments exist in the literature. However, observational catalogues of walls are not yet available and so, walls are currently defined from a primarily theoretical perspective (e.g. Hertzsch et al. (2025)). In our framework, filaments are not explicitly identified and they tend to emerge, specifically, at the intersections of two or more walls. As a result, walls and filaments are treated as a single structural category (i.e. walls and filaments), for which no direct observational counterpart currently exists.

5.4. Impact and possible improvements

This simulator presents several advantages, compared with other methods. First, it allows us to handle key spatial characteristics of each structure, such as the density of galaxies within each structure and its spatial position, allowing for the construction of standard mock catalogues or even the generation of edge-case scenarios by changing parameters to extreme values (e.g. the impact of changing the number of voids to unrealistic values, as shown in Fig. D.6). Second, each galaxy has a unique single label, meaning that the classification has a unique solution; thus, allowing us to avoid the possibility of finding multiple minima for one class. Third, the definition of the structures is consistent across the dataset, regardless of the position and orientation of each structure, the distance to the observer, or the Malmquist bias, thereby improving the generalisation of models. Finally, multiple numbers of different universes can be generated by changing the random seed, which is decisive for increasing the generalisation ability of ML models and, thus, decreasing the overfitting.

Given these advantages, several LSS analysis methods would benefit from the flexibility of the present simulator. For instance, Aragon-Calvo (2019) generates a Voronoi tessellation to represent the LSS and performs its classification. However, instead of populating each structure with galaxies, the space is voxelised and then entered to the convolutional neural network (CNN). This makes the method highly dependent on the chosen voxel size, imposing a classification based on the galaxies found within each classified voxel, regardless of whether they belong to different structures (block classification). Using these mock universes, the first layers of the CNN can be redesigned, making it able to process each galaxy independently, and assigning a structure to each one, regardless of the voxel size or other imposed spatial parameter.

Besides these benefits, there are several improvements that can be adopted in the present work to generate more realistic datasets. For example, walls and filaments are generated in a way that makes them extremely straight; whereas in the SDSS catalogue, these structures clearly have a more organic form, with irregularly shaped walls and curvy filaments. These shapes can be achieved by expanding and shrinking the 3D space in the centres of voids, randomly. This action can give random concave and convex shapes to both walls and filaments. In addition, this simulator cannot generate wall and filament galaxies independently. The implementation of this feature is crucial to encourage the implementation of wall and filament galaxy classification algorithms using this simulator as reference to measure their accuracies. Nevertheless, this simulator is now ready to be used against the extensive list of existing LSS classification algorithms, taking as an example, those presented in Libeskind et al. (2018).

6. Summary and conclusions

We present a novel geometrical mock galaxy catalogue generator, where its simulated galaxies follow the statistical behaviour of the observed ones in each respective LSS of the Universe in which they reside. The proposed simulator enables a precise customisation of structural properties, unambiguous labelling, and consistency under varying observational conditions. In addition, the variability introduced by random seeds enhances data generalisation (crucial to reduce overfitting in ML and DL models). As a use case, the simulator was fine-tuned to mimic the galaxies found in the SDSS catalogue. To this end, several observational studies characterising the galactic properties based on

structure have been taken into account, such as [Pan et al. \(2012\)](#) for voids and [Tempel et al. \(2017\)](#) for clusters. It is not only the purely structural properties that are included in the simulation, but also the observational biases such as the FoG effect and the Malmquist bias are taken into account. Among other parameters, these characteristics are fully customisable. In this specific use case, the following results were obtained:

- In each simulation, a full-sky mock catalogue was generated, which was then sliced into six parts where each one spread 120° in R.A. and 90° in Dec., equivalent to the area covered by the SDSS footprint.
- Given the standard configuration, each slice of the mock catalogues presents a total number of $\sim 500,000$ galaxies, distributed on the basis of their affiliated structure, where $\sim 3\%$ of galaxies belong to clusters, $\sim 81\%$ of galaxies belong to walls and filaments, and $\sim 16\%$ belong to voids. In terms of volume, the clusters, walls and filaments, and voids represent 0.07% , $\sim 19\%$, and $\sim 81\%$ of the whole simulation volume, respectively.
- The slices of the studied mock catalogue has $16,406 \pm 832$, $403,150 \pm 7643$ and $79,387 \pm 3272$ galaxies distributed in 333 ± 17 , $15,022 \pm 569$ and 1060 ± 37 clusters, walls or filaments and cosmic voids, respectively.
- These results are consistent with those observed in the SDSS catalogue ([Pan et al. 2012](#); [Tempel et al. 2017](#)), which is expected due to the construction of the mock universe.

In conclusion, this simulator provides a robust and expandable platform for building customisable mock universe catalogues. It enables a systematic testing of LSS classification methodologies, supports the development of ML approaches for galaxy surveys, and facilitates controlled explorations of boundary-case scenarios. These mock catalogues can be used to train ML models and evaluate their accuracy, which will be the subject of a future work.

Data availability

The source code of the presented simulator is open source and publicly available at: <https://gitlab.com/astrogal/mocklss>.

Acknowledgements. We dedicate this work to the memory of our dearest colleague and friend J. Jiménez-Vicente. The authors thank the anonymous referee for the thorough reading and constructive feedback. The CAVITY project acknowledges financial support by the research projects AYA2017-84897-P, PID2020-113689GB-I00, PID2020-114414GB-I00, and PID2023-149578NB-I00 funded by the Spanish Ministry of Science and Innovation (MCIN/AEI/10.13039/501100011033) and by FEDER/UE; the project A-FQM-510-UGR20 funded by FEDER/Junta de Andalucía-Consejería de Transformación Económica, Industria, Conocimiento y Universidades/Proyecto; by the grants P20-00334 and FQM108, funded by Junta de Andalucía; and by Consejería de Universidad, Investigación e Innovación (Junta de Andalucía) and Gobierno de España and European Union NextGenerationEU through grant AST22_44. M.A-F. acknowledges support from the Emergia program (EMERGIA20-38888) from Consejería de Transformación Económica, Industria, Conocimiento y Universidades of the Junta de Andalucía. Funding for SDSS-III has been provided by the Alfred P. Sloan Foundation, the Participating Institutions, the National Science Foundation, and the U.S. Department of Energy Office of Science. SDSS-III is managed by the Astrophysical Research Consortium for the Participating Institutions of the SDSS-III Collaboration including the University of Arizona, the Brazilian Participation Group, Brookhaven National Laboratory, Carnegie Mellon University, University of Florida, the French Participation Group, the German Participation Group, Harvard University, the Instituto de Astrofísica de Canarias, the Michigan State/Notre Dame/ JINA Participation Group, Johns Hopkins University, Lawrence Berkeley National Laboratory, Max Planck Institute for Astrophysics, Max Planck Institute for Extraterrestrial Physics, New Mexico State University, New York University, Ohio State University, Pennsylvania State University, University of Portsmouth, Princeton

University, the Spanish Participation Group, University of Tokyo, University of Utah, Vanderbilt University, University of Virginia, University of Washington, and Yale University. The SDSS-III web site is <http://www.sdss3.org>. We are also grateful for the computing resources and related technical support provided by PROTEUS, the supercomputing centre of Institute Carlos I in Granada, Spain. This research made use of [Python Core Team \(2019\)](#) v3.11 programming language. This work made use of [Astropy \(<http://www.astropy.org>\)](#) a community- developed core Python package and an ecosystem of tools and resources for astronomy ([Astropy Collaboration et al. 2013, 2018, 2022](#)); [SciPy \(\[Virtanen et al. 2020\]\(http://www.virtanen.org\)\)](#); [Numpy \(\[Harris et al. 2020\]\(http://www.harris.org\)\)](#); and [Pandas \(\[pandas development team 2020\]\(http://www.pandas.org\); \[McKinney 2010\]\(http://www.mckinney.org\)\)](#).

References

Abazajian, K. N., Adelman-McCarthy, J. K., Agüeros, M. A., et al. 2009, *ApJS*, 182, 543
 Abell, G. O., Corwin, Jr., H. G., & Olowin, R. P. 1989, *ApJS*, 70, 1
 Alam, S., Albareti, F. D., Allende Prieto, C., et al. 2015, *ApJS*, 219, 12
 Alpaslan, M., Robotham, A. S. G., Driver, S., et al. 2014, *MNRAS*, 438, 177
 Aragón Calvo, M. A. 2007, PhD thesis, University of Groningen, Netherlands
 Aragón-Calvo, M. A. 2019, *MNRAS*, 484, 5771
 Aragón-Calvo, M. A., Platen, E., van de Weygaert, R., & Szalay, A. S. 2010, *ApJ*, 723, 364
 Argudo-Fernández, M., Duarte Puertas, S., Ruiz, J. E., et al. 2017, *PASP*, 129, 058005
 Astropy Collaboration, Price-Whelan, A. M., Lim, P. L., et al. 2022, *ApJ*, 935, 167
 Astropy Collaboration, Price-Whelan, A. M., Sipőcz, B. M., et al. 2018, *AJ*, 156, 123
 Astropy Collaboration, Robitaille, T. P., Tollerud, E. J., et al. 2013, *A&A*, 558, A33
 Balogh, M., Eke, V., Miller, C., et al. 2004, *MNRAS*, 348, 1355
 Balogh, M. L., Schade, D., Morris, S. L., et al. 1998, *ApJ*, 504, L75
 Cautun, M., van de Weygaert, R., Jones, B. J. T., & Frenk, C. S. 2014, *MNRAS*, 441, 2923
 Colless, M., Dalton, G., Maddox, S., et al. 2001, *MNRAS*, 328, 1039
 Douglass, K. A., Veyrat, D., & BenZvi, S. 2023, *ApJS*, 265, 7
 Dressler, A. 1980, *ApJ*, 236, 351
 Driver, S. P., Hill, D. T., Kelvin, L. S., et al. 2011, *MNRAS*, 413, 971
 Einasto, J. 1965, *Trudy Astrofizicheskogo Instituta Alma-Ata*, 5, 87
 El-Ad, H. & Piran, T. 1997, *ApJ*, 491, 421
 El-Ad, H., Piran, T., & da Costa, L. N. 1996, *ApJ*, 462, L13
 García-Benito, R., Jiménez, A., Sánchez-Menguiano, L., et al. 2024, *A&A*, 691, A161
 Geller, M. J. & Huchra, J. P. 1989, *Science*, 246, 897
 Gott, III, J. R., Jurić, M., Schlegel, D., et al. 2005, *ApJ*, 624, 463
 Guzzo, L., Scoggio, M., Garilli, B., et al. 2014, *A&A*, 566, A108
 Harris, C. R., Millman, K. J., van der Walt, S. J., et al. 2020, *Nature*, 585, 357
 Hertzsch, B., Feldbrugge, J., Rodriguez, M., & van de Weygaert, R. 2025, arXiv e-prints, arXiv:2510.02419
 Icke, V. & van de Weygaert, R. 1987, *A&A*, 184, 16
 Jaber, M., Peper, M., Hellwing, W. A., Aragón-Calvo, M. A., & Valenzuela, O. 2024, *MNRAS*, 527, 4087
 Kreckel, K., Platen, E., Aragón-Calvo, M. A., et al. 2011, *AJ*, 141, 4
 Le Fèvre, O., Vettolani, G., Garilli, B., et al. 2005, *A&A*, 439, 845
 Lewis, I., Balogh, M., De Propris, R., et al. 2002, *MNRAS*, 334, 673
 Libeskind, N. I., van de Weygaert, R., Cautun, M., et al. 2018, *MNRAS*, 473, 1195
 Mao, Q., Berlind, A. A., Scherrer, R. J., et al. 2017, *ApJ*, 835, 161
 McKinney, W. 2010, in *Proceedings of the 9th Python in Science Conference*, ed. S. van der Walt & J. Millman, 51 – 56
 Navarro, J. F., Frenk, C. S., & White, S. D. M. 1996, *ApJ*, 462, 563
 Navarro, J. F., Frenk, C. S., & White, S. D. M. 1997, *ApJ*, 490, 493
 Neyrinck, M. C. 2008, *MNRAS*, 386, 2101
 O’Kane, C. J., Kuchner, U., Gray, M. E., & Aragón-Salamanca, A. 2024, *MNRAS*, 534, 1682
 Pan, D. C., Vogeley, M. S., Hoyle, F., Choi, Y.-Y., & Park, C. 2012, *MNRAS*, 421, 926
 pandas development team, T. 2020, *pandas-dev/pandas: Pandas*
 Pérez, I., Verley, S., Sánchez-Menguiano, L., et al. 2024, *A&A*, 689, A213
 Pimbblet, K. A., Drinkwater, M. J., & Hawkrigg, M. C. 2004, *MNRAS*, 354, L61
 Python Core Team. 2019, *Python: A dynamic, open source programming language*, Python Software Foundation
 Rines, K., Geller, M. J., Kurtz, M. J., & Diaferio, A. 2005, *AJ*, 130, 1482
 Seth, R. & Raychaudhury, S. 2020, *MNRAS*, 497, 466
 Sparke, L. S. & Gallagher, III, J. S. 2007, *Galaxies in the Universe: An Introduction* (Cambridge, UK: Cambridge University Press)
 Tempel, E., Stoica, R. S., Martínez, V. J., et al. 2014a, *MNRAS*, 438, 3465
 Tempel, E., Tago, E., & Liivamägi, L. J. 2012, *A&A*, 540, A106
 Tempel, E., Tamm, A., Gramann, M., et al. 2014b, *A&A*, 566, A1
 Tempel, E., Tuvikene, T., Kipper, R., & Libeskind, N. I. 2017, *A&A*, 602, A100
 van de Weygaert, R. & Icke, V. 1989, *A&A*, 213, 1
 Van Kempen, W., Cluver, M., Jarrett, T., et al. 2024, *PASA*, 41, e096
 Virtanen, P., Gommers, R., Oliphant, T. E., et al. 2020, *Nature Methods*, 17, 261
 York, D. G., Adelman, J., Anderson, Jr., J. E., et al. 2000, *AJ*, 120, 1579

Appendix A: Default simulator parameters (SDSS-like)

Table A.1. Parameters considered in this work for the SDSS-like simulation.

Default simulator configuration		Value	Unit
Parameter			
General configuration			
Seed	Random number based on hour and date		
Number of voids	8089	Voids	
Maximum diameter of simulated universe	1000	$[h^{-1}Mpc]$	
Number of CPU cores	Maximum of the host machine		
Malmquist bias	True	Boolean	
Reference catalogue	Alam et al. (2015)		
Grid size for volume calculation	5	$[h^{-1}Mpc]^3$	
Clusters			
FoG bias	True	Boolean	
Number of galaxies prob. distribution	SDSS		
Number of galaxies SDSS prob. distribution	$P_{n_i, C_i}(x) = (2233.15 \times e^{-x/15.03} + 0.97)/4822.5$		
Minimum number of galaxies per cluster	30	galaxies	
Maximum number of galaxies per cluster	300	galaxies	
Maximum radius prob. distribution	SDSS (fixed, depending on # of gal. in cluster: n_i)		
Maximum radius SDSS formula	$R_{max, C_i}(n_i) = n_i^{1/3.32}/2.59$	$[h^{-1}Mpc]$	
Minimum radius	1	$[h^{-1}Mpc]$	
Maximum radius	4	$[h^{-1}Mpc]$	
Radial velocity dispersion	$\sigma_v = -585.40e^{-n_i/59.49} + 804.71$	km/s	
Walls & filaments			
Wall galaxy density	0.18	galaxies $\times (h^{-1}Mpc)^{-2}$	
Minimum wall surface	0	$[h^{-1}Mpc]^2$	
Maximum wall surface	2000	$[h^{-1}Mpc]^2$	
Galaxy spatial distribution within a wall	Gaussian		
Galaxy spatial distribution mean	$\mu = 0$	$[h^{-1}Mpc]$	
Galaxy spatial distribution dispersion	$\sigma = 0.5$	$[h^{-1}Mpc]$	
Voids			
Grid size for low density zones detection	5	$[h^{-1}Mpc]^3$	
Determination of number of galaxies	By ratio (depending on other structures)		
Number of galaxies ratio	$N_{void, gal.} = 0.116 \times (N_{cl, gal.} + N_{w, \& f, gal.})$	galaxies	

Appendix B: Results of a simulation given the default configuration

Table B.1. Analysis of the slices of the studied mock universe.²

Parameter	Simulated value	Ref. catalogue value	Unit
General characteristics			
Random seed	20251211082334		
Reference catalogue		Alam et al. (2015)	
Number of galaxies (common footprint ³)	$275,487 \pm 6700$	274,975	galaxies
R.A. range (R.A. max. - R.A. min.)	120	152.05	[$^{\circ}$]
DEC range (DEC max. - DEC min.)	90	73.99	[$^{\circ}$]
Mean density of galaxies (common footprint)	0.0057 ± 0.0001	0.005	galaxies $\times (h^{-1}Mpc)^{-3}$
Clusters			
Reference catalogue		Tempel et al. (2017)	
Number of cluster galaxies	$16,406 \pm 832$	16,419	galaxies
Number of clusters	333 ± 17	322	clusters
Min. n° of galaxies within a cluster	30	30	galaxies
Max. n° of galaxies within a cluster	291	254	galaxies
Density of galaxies within clusters	0.27 ± 0.01		galaxies $\times (h^{-1}Mpc)^{-3}$
Clusters connectivity (node degree)	4		filaments / node
Walls & filaments			
Number of wall and filament galaxies	$403,150 \pm 7643$		galaxies
Number of walls	$15,022 \pm 569$		walls
Density of galaxies within walls and filaments	0.023 ± 0.001		galaxies $\times (h^{-1}Mpc)^{-3}$
Walls surface	516.34 ± 504.89		$(h^{-1}Mpc)^2$
Filaments length	31.18 ± 27.16		$h^{-1}Mpc$
Voids			
Reference catalogue		Pan et al. (2012)	
Number of void galaxies	$79,387 \pm 3272$	79,947	galaxies
Number of voids	1060 ± 37	1054	voids
Density of galaxies within voids	0.0010 ± 0.0001		galaxies $\times (h^{-1}Mpc)^{-3}$
Median effective radius	28.61 ± 11.28	17-25	$h^{-1}Mpc$
Number of adjacent walls	14.28 ± 7.15		walls / void
Number of adjacent filaments	39.78 ± 10.89		filaments / void
Number of adjacent nodes	26.95 ± 6.94		nodes / void
Void shape ⁴	1.28 ± 0.35		dimensionless

² The symbol " \pm " represents the standard deviation of measured values (1σ)

³ This number is measured in a chosen footprint for with both mock and reference catalogues present main data without border effects. The selected footprint limits are: $RA \in [140^{\circ}, 230^{\circ}]$, $DEC \in [0^{\circ}, 50^{\circ}]$ and $Dist. \in [100, 500][h^{-1}Mpc]$

⁴ Void shape was computed for each void as the fraction between the sum of the surface of its surrounding walls and the area of a sphere whose $r = R_{eff}$.

Appendix C: Density of galaxies along cluster radius

Spatial distribution of galaxies along the cluster radius is highly inhomogeneous. For instance, consider a cluster with n galaxies, where its furthest galaxy is at ~ 2 Mpc from its geometrical centre, and the spatial distribution of galaxies along its radius follows a Gaussian distribution, centred in $r = \mu = 0$ Mpc and with a standard deviation of $\sigma = \sim \frac{2}{3}$ Mpc. In this example, three slices (or ‘shells’) were studied according to several ranges of radial distances in the cluster: i) from the centre ($r_0=0$ Mpc) to 1σ ($r_1=0.66$ Mpc); ii) from 1σ ($r_1=0.66$ Mpc) to 2σ ($r_2=1.32$ Mpc); and iii) from 2σ ($r_2=1.32$ Mpc) to 3σ ($r_3=2$ Mpc). In Table C.1, the inner and outer radii (columns 2 and 3 respectively) of each studied shell, its galaxy proportion (column 4), its volume (column 5) and its galaxy density (column 6) are shown. In the last row of Table C.1 the total number of galaxies inside the cluster and its total volume is considered, giving us a mean density that matches with the previously calculated one. The densities within the shells vary by several orders of magnitude, making it inappropriate to determine or apply an average galaxy density for clusters given their spatial distribution.

Table C.1. Galaxy densities versus radial slices for cluster structures.

Shell	Inner radius	Outer radius	Galaxies	Volume	Density
	Mpc	Mpc	%	$[h^{-1} \text{Mpc}]^3$	$[\frac{\text{galaxies}}{(h^{-1} \text{Mpc})^3}]$
i	0.00	0.66	68.3	1.20	$0.570n$
ii	0.66	1.32	27.2	8.43	$0.032n$
iii	1.32	2.00	4.2	23.88	$0.0017n$
Total	0.00	2.00	99.7	33.51	$0.0298n$

Notes. n represents the number of galaxies within the cluster. In the example, $n = \text{Total mass of cluster}/\text{Mean galaxy mass} = 10^{14} M_\odot/10^{11} M_\odot = 1000$ [galaxies].

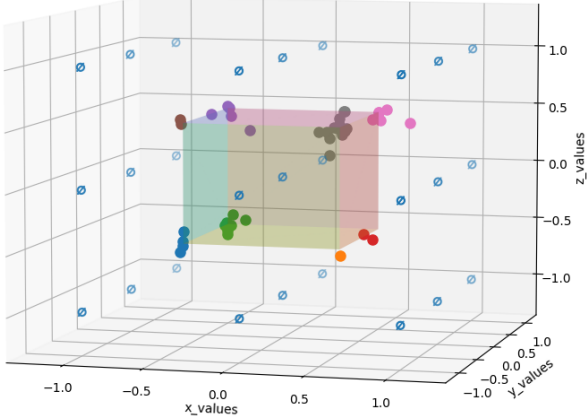


Fig. D.1. Voronoi 3D generated central cube region. The random cluster galaxies grow around the vertices, acting as the centroid of each cluster. The empty symbols are the simulated seeds of voids. The points represent simulated cluster galaxies coloured depending on their belonging cluster.

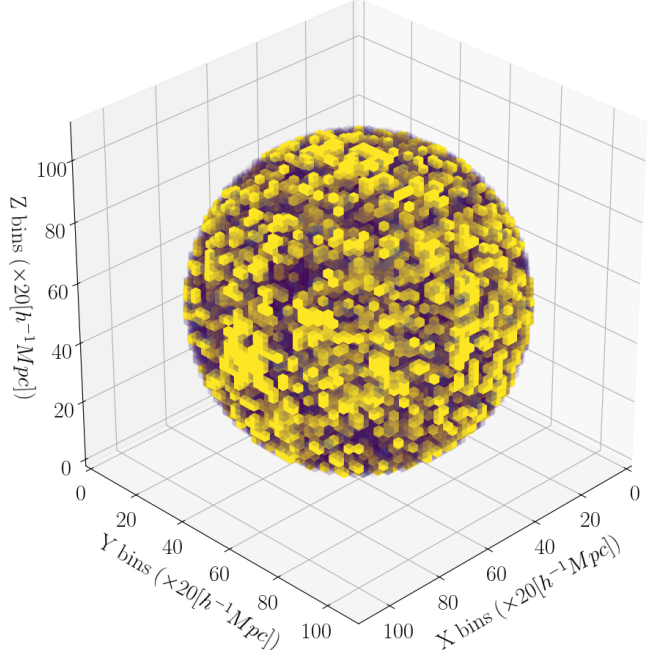


Fig. D.3. 3D example of a void galaxies probability map, generated by inverting a 3D histogram performed over the galaxies from other structures. Yellowish and violetish voxels represents a spatial region with the highest and lowest probability of generating void galaxies, respectively. The size of the voxels was oversized to $20[h^{-1}\text{Mpc}]^3$ for a clearer representation.

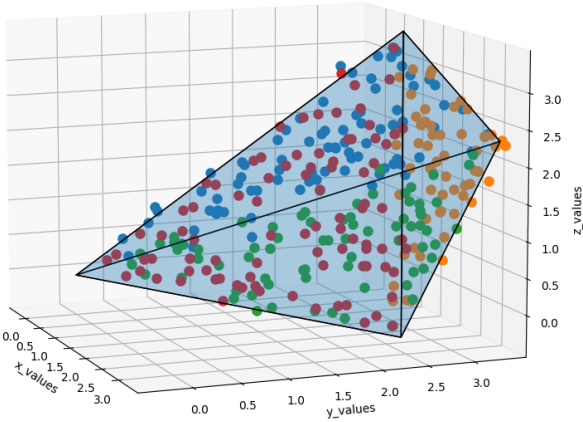


Fig. D.2. Example of a region from a Voronoi 3D tessellation with its faces populated with random points representing wall and filament mock galaxies. Extracted planes from the Voronoi tessellation, interpreted as cosmic wall (blue faces), extracted edges from the Voronoi tessellation, interpreted as cosmic filaments (black lines), and simulated wall galaxies coloured depending on their belonging wall (coloured points).

Appendix D: Additional figures

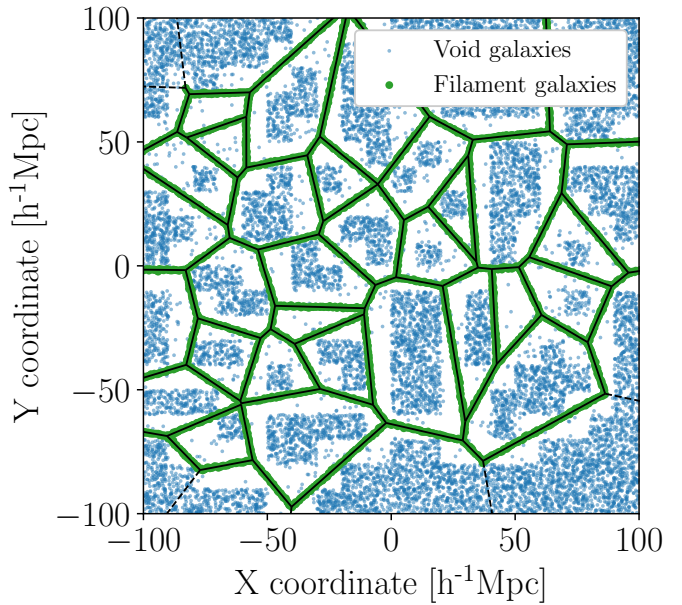


Fig. D.4. 2D example of the under-dense areas in the void galaxies generation method. The figure shows a Voronoi tessellation of a surface. Black lines represents the filaments which were populated with galaxies (green dots). Blue dots represents generated uniformly distributed void galaxies. The threshold was exaggerated to highlight how the algorithm skips areas previously populated with galaxies from other structures.

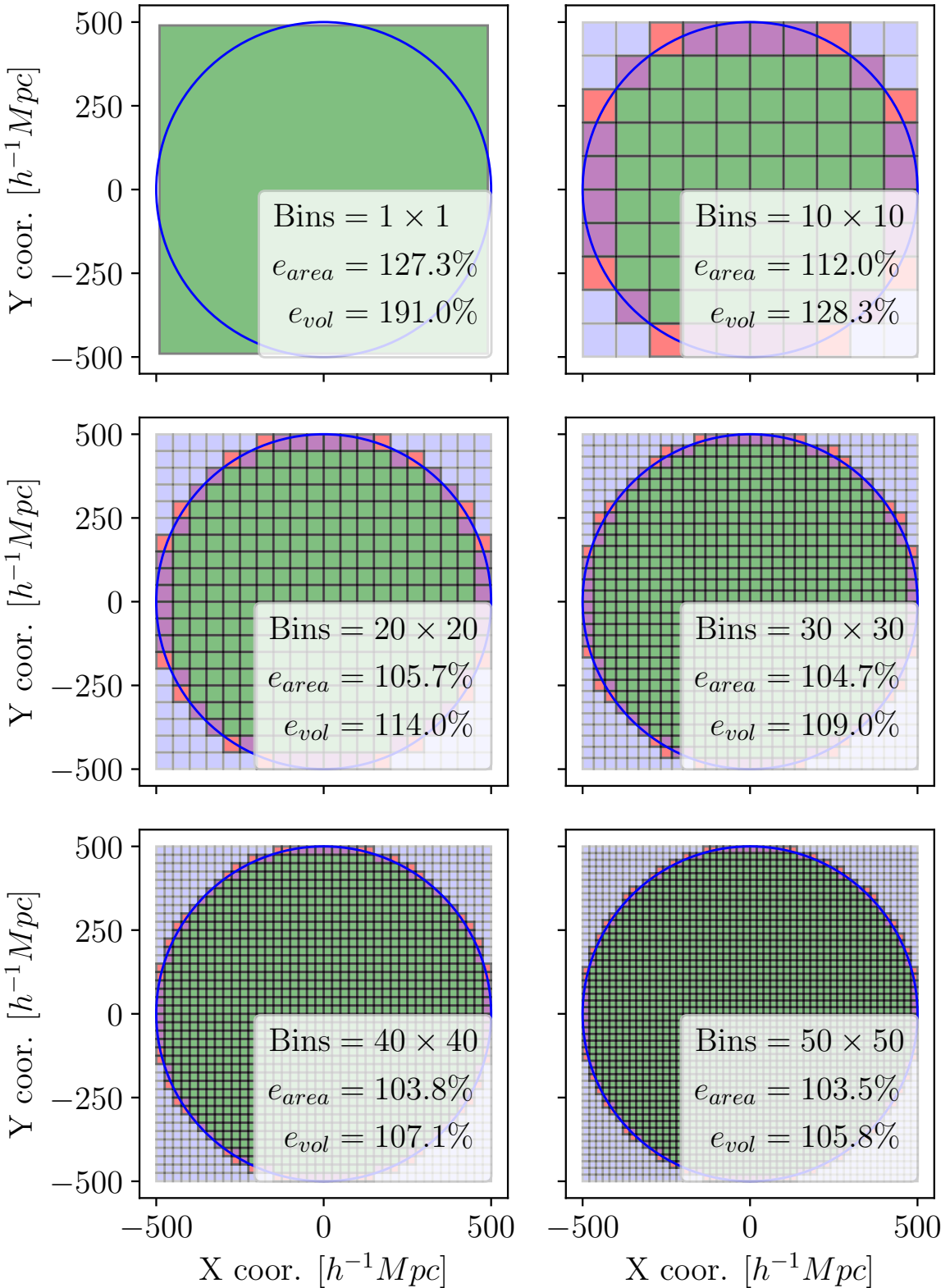


Fig. D.5. Effect of sampling the sphere volume using different voxel sizes. The figure shows a 2D representation of the simulated spherical universe (blue circle). The voxel volume method will divide the space in voxels, represented as coloured squares. Those voxels which their centres are further than the simulated universe radius ($500 [h^{-1} Mpc]$ in this example) will not be processed, represented in light blue. The remaining voxels will be taken into account to compute the volume of the structures. While inner voxels present no problem (green ones), frontier voxels are adding more volume erratically because cubes cannot precisely fit the surface of a sphere. While purple voxels add small errors, red voxels are adding the expected volume twice or more for that zone. This 2D example shows how the proportion between the computed and theoretical areas (represented by e_{area}) decreases proportionally with the bin size. In 3D, it occurs in the same way with computed and theoretical volumes, represented by e_{vol} .

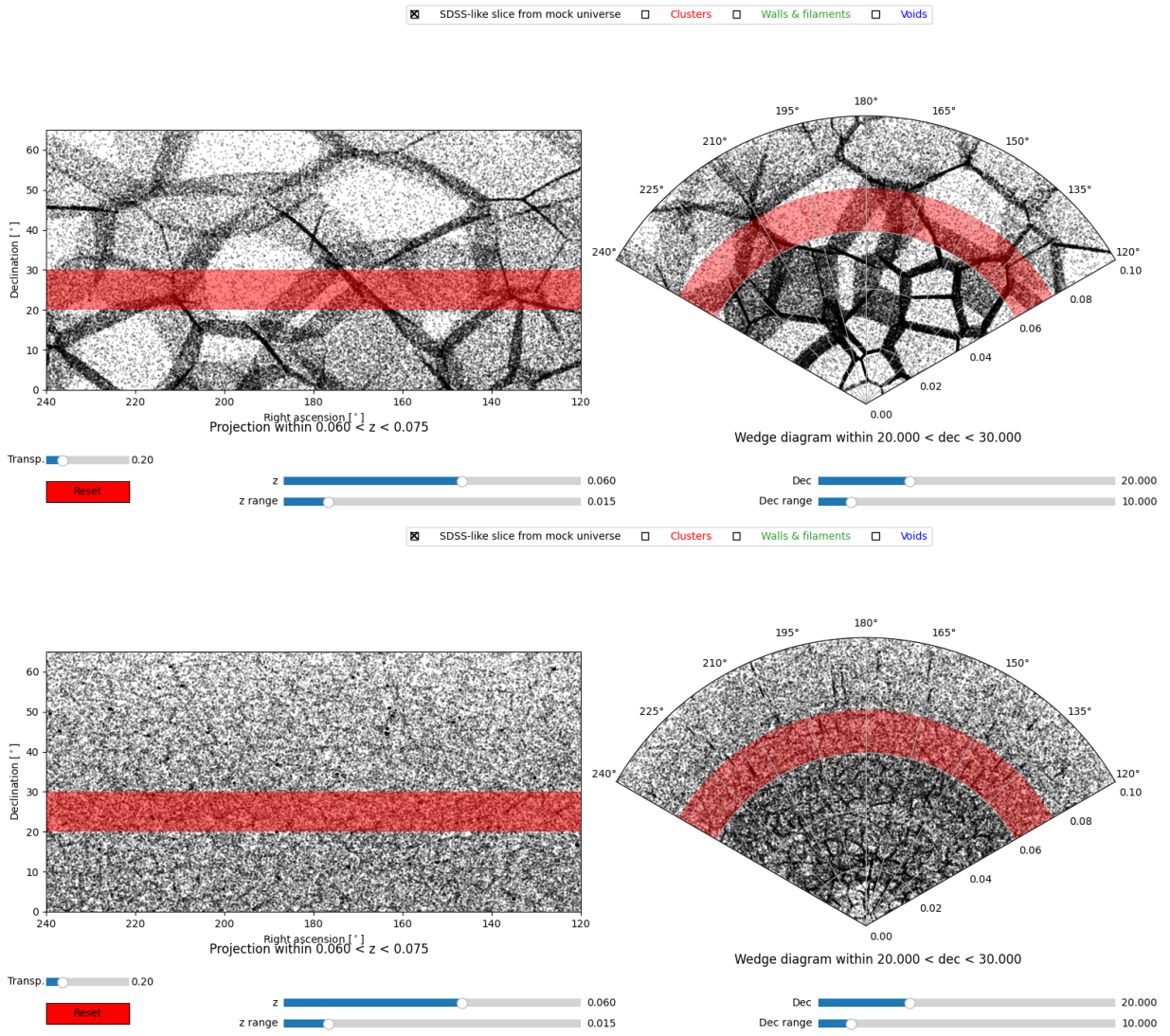


Fig. D.6. SDSS-like slice II from two randomly generated mock universes with ten times fewer (upper panel) and ten times more (lower panel) voids than in default configuration. In both panels, the red stripes represent the range of redshift and declination shown in the other sub-panel.